

# Spin–spin coupling between the two unpaired electrons in cross-conjugated tetrathiafulvalene dication radicals

Jun Yamauchi,<sup>1\*</sup> Takuo Aoyama,<sup>1</sup> Katsuichi Kanemoto,<sup>1</sup> Shigeru Sasaki<sup>2</sup> and Masahiko Iyoda<sup>2</sup>

<sup>1</sup>Graduate School of Human and Environmental Studies, Kyoto University, Nihonmatsu, Yoshida, Kyoto 606-8501, Japan

<sup>2</sup>Department of Chemistry, Graduate School of Science, Tokyo Metropolitan University, Hachioji, Tokyo 192-0397, Japan

Received 10 September 1999; revised 16 November 1999; accepted 20 November 1999

**ABSTRACT:** Spin–spin interactions were examined for bis(tetrathiafulvalenyl) (TTF) derivatives bridged with a 1,1-vinyl group (2,2-diphenyl, **1**; 2,2-fluorenylidene, **2**; and 2,2-dimethyl, **3**). The chemical oxidation of these cross-conjugated TTFs using AgClO<sub>4</sub> yielded characteristic seven-line ESR spectra, indicating the exchange interactions between the unpaired electrons on each TTF moiety. Compounds **2** and **3**, in addition, exhibited fine structures and half-field resonances in the frozen solutions, which evidence the triplet interaction in the solid state, even with a twisted geometry of the molecular configuration. These findings substantiate the possibility of spin–spin interactions or triplet ground states predicted for some TTF oligomers. Copyright © 2000 John Wiley & Sons, Ltd.

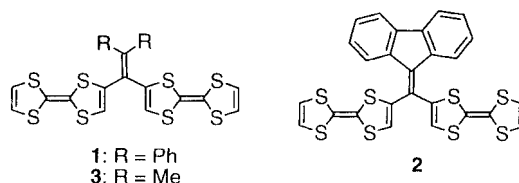
**KEYWORDS:** dimeric TTF; cation radical; x-ray structure analysis; cyclic voltammetry; ESR; spin–spin interaction

## INTRODUCTION

Much attention has recently been paid to novel molecule-based materials leading toward synthetic organic conductors and ferromagnets.<sup>1</sup> Some of the strategic systems of those electric and magnetic properties have been closely concerned with charge-transfer complexes since the discovery of the highly conducting complex of tetrathiafulvalene (TTF) and 7,7,8,8-tetracyanoquinodimethane (TCNQ).<sup>2</sup> A promising class of donors is derived from the tetrachalcogenafulvalene moiety. New donors based on the parent TTF moiety have been extensively pursued for molecular organic conductors and ferromagnets,<sup>3</sup> and oligomeric TTFs have been also developed for increased dimensionality of the conducting process or magnetic interaction.<sup>4</sup> Recent modifications of TTF have placed emphasis on the preparation of dimeric TTFs as new electron donors.<sup>5</sup> In addition, theoretical calculations on TTF dimers or oligomers have shed light on the spin–spin interactions between the unpaired electrons in the dication of the TTF dimers, especially the parallel spin ground state in some cases.<sup>6</sup> These kinds of investigations stem from a semiempirical study of electron exchange interactions in organic high-spin  $\pi$  systems.<sup>7</sup> Thus, synthetic and well-characterized examinations have attracted much interest in these materials.

Based on a theoretical prediction, bis(tetrathiafulvalenyl) derivatives bridged with a carbonyl group were

synthesized, and their dication radical states were checked by cyclic voltammetry (CV) and electron spin resonance (ESR) measurements.<sup>8</sup> The study concluded that the spin–spin coupling between the two unpaired electrons is strongly dependent on the geometry of the two TTFs and that, in frozen solutions, spin–spin interaction occurred to produce the biradical, but the ground state was a singlet, which was not in agreement with the prediction of a triplet ground state on the basis of the theoretical calculations. Tentative explanations are as follows.<sup>7</sup> Oxyallyl may possess a substantial HOMO–LUMO gap due to oxygen-perturbed selective lowering of the symmetrical  $\pi$  orbital, and the carbonyl group is likely to contain an ionic polar structure which will result in less spin–spin interaction due to reduced  $\pi$  overlap. Therefore, we tried another type of dimeric TTFs and provided a preliminary report of the synthesis of bis(tetrathiafulvalenyl)ethylenes, together with some properties of their dication radical salts.<sup>9</sup> In this paper, we detail the spin–spin interactions of the dications derived from bis(tetrathiafulvalenyl)ethylenes **1–3** (Scheme 1).



Scheme 1

\*Correspondence to: J. Yamauchi, Graduate School of Human and Environmental Studies, Kyoto University, Nihonmatsu, Yoshida, Kyoto 606-8501, Japan.

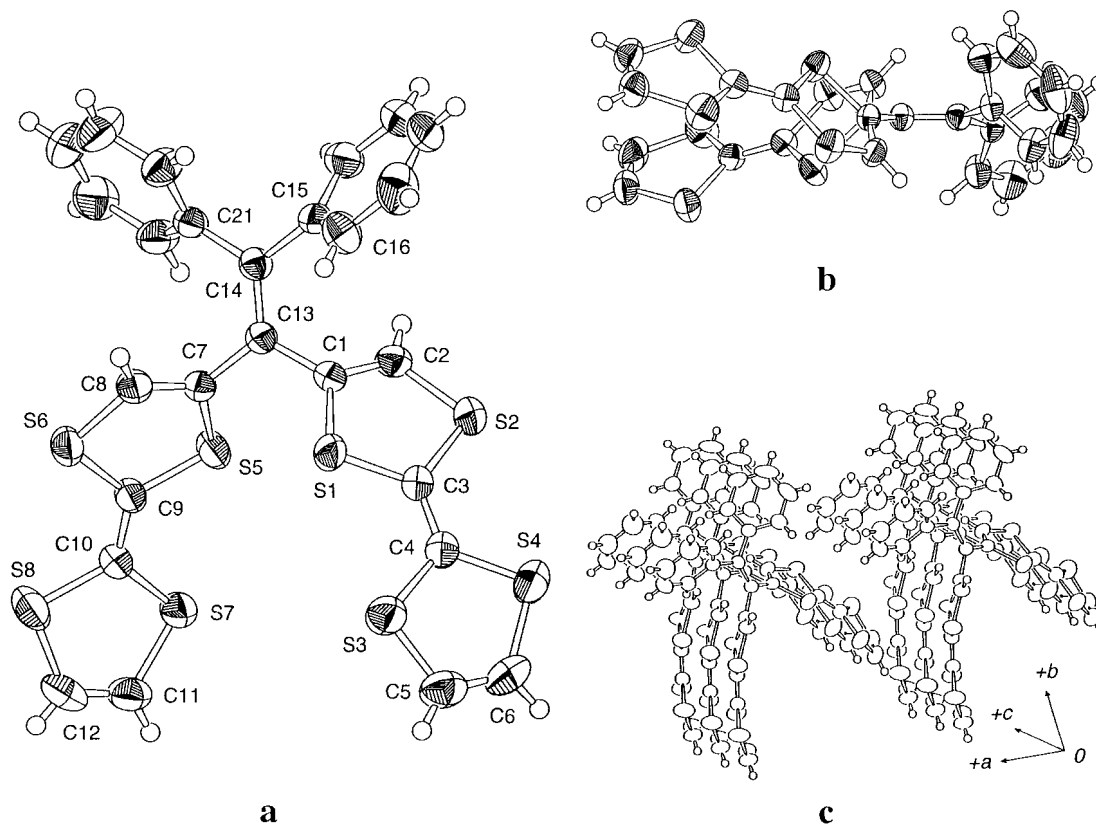


**Figure 1.** ORTEP plots of 2,2-bis(tetrathiafulvalenyl)-1,1-diphenylene (**1**). (a) Top view of the molecule; (b) view perpendicular to that shown in (a); (c) crystal structure

## RESULTS AND DISCUSSION

### Molecular structure of **1**

The molecular structure and packing diagram of the neutral donor **1** were determined by x-ray analysis (Fig. 1). As shown in Fig. 1(a), the two TTF parts in **1** are oriented in a twisted conformation, and the dihedral angles of the two TTF parts to the ethylene bridge are  $49.3^\circ$  and  $51.4^\circ$ . In a similar manner, the two phenyl groups show a twisted conformation, the dihedral angles to the ethylene being  $44.6^\circ$  and  $55.5^\circ$ . The bond distances and angles in the TTF and phenyl parts of the molecule have normal values. Interestingly, the two  $sp^2$  carbons in the ethylene bridge exhibit a small twisting [Fig. 1(b)], reflecting its overcrowded double bond (the dihedral angle between C1—C13—C7 and C15—C14—C21 is  $11^\circ$ ). Although the crystal structure shows a stacking of the TTF and phenyl rings, there is no S...S interaction between the two neighboring TTF rings [Fig. 1(c)].

### Cyclic voltammogram

In order to estimate the donor ability and the interaction between the two TTF moieties in **1–3**, the redox potentials of these donors were measured by CV (Table

1). All 1,1-bis(tetrathiafulvalenyl)ethylenes show two reversible two-electron redox waves. As shown in Fig. 2, the cyclic voltammogram of **1** corresponds to two discrete two-electron transfer processes. Although dimeric TTF molecules generally display the multi-step redox behavior shown in Scheme 2, the interaction between the two TTF parts in **1** seems weak owing to the cross-conjugated character. In addition, CV sometimes gives no splitting of potentials when two or three redox potentials become so closely spaced together as to be practically continuous. In the case of bis(tetrathiafulvalenyl)ketone, four redox potentials ( $E_{1/2} = 0.58, 0.67, 1.01$  and  $1.05$  V vs SCE) were observed, and the first two redox potentials were slightly more positive than the first redox potential of TTF.<sup>8</sup> In our case, however, molecules **1–3** exhibit only two redox peaks (Table 1), although the

**Table 1.** Cyclic voltammetric data for **1–3** and TTF<sup>a</sup>

Compound	$E^1_{1/2}$ (V)	$E^2_{1/2}$ (V)	$\Delta E$ (V)
TTF	0.36	0.73	0.37
<b>1</b>	0.40	0.79	0.39
<b>2</b>	0.45	0.80	0.35
<b>3</b>	0.39	0.72	0.33

<sup>a</sup>  $n\text{-Bu}_4\text{NClO}_4$  (0.1 M) in anhydrous benzonitrile at  $23^\circ\text{C}$ ; Pt working and counter electrodes. Potentials were measured against an  $\text{Ag}/\text{Ag}^+$  reference electrode and converted to the value vs SCE.

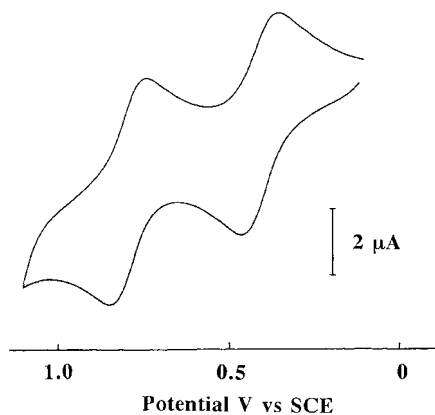
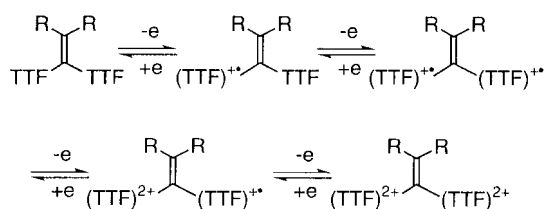


**Figure 2.** Cyclic voltammogram of **1** (benzonitrile, 20°C, *n*-Bu<sub>4</sub>NClO<sub>4</sub> electrolyte, Pt electrode, scan rate 100 mV s<sup>-1</sup>)

first redox potentials ( $E_{1/2}^1 = 0.39\text{--}0.45$  V vs SCE) of **1–3** correspond well with that of TTF under the same conditions ( $E_{1/2}^1 = 0.36$  V vs SCE). These resolved and unresolved cyclic voltammograms have been exemplified with many dimeric TTF molecules.<sup>5</sup> Donor **2** shows a slightly larger oxidation potential ( $E_{1/2}^1 = 0.45$  V vs SCE) as compared with those of **1** and **3** ( $E_{1/2}^1 = 0.39$  and 0.40 V vs SCE), presumably owing to the electron-withdrawing effect of its fluorenylidene group. On the basis of the redox potentials, it can be expected that even weak oxidizing agents would readily yield doubly oxidized species of **1–3**.

### ESR spectra and spin–spin interactions

Figure 3 shows a hyperfine (hf) spectrum of **1**, together with large amplified spectra ( $\times 50$ ) on either side of the magnetic field. The hf lines in the center, which include seven lines with an intensity ratio of ca 1:6:15:20:15:6:1, are caused by six essentially equivalent protons of the two substituted TTFs. The hf coupling constant (hfcc) was found to be 0.06 mT, which is almost half of that of the TTF monocation radical.<sup>2,10</sup> The spectral pattern, therefore, substantiates a substantial spin–spin coupling between the two unpaired electrons on each TTF moiety, that is, a fast exchange rate compared with the ESR observation frequency (X-band). (The ESR pattern and the magnitude of the hfcc observed here can also be explained on the basis of one-electron delocalization on



**Scheme 2**

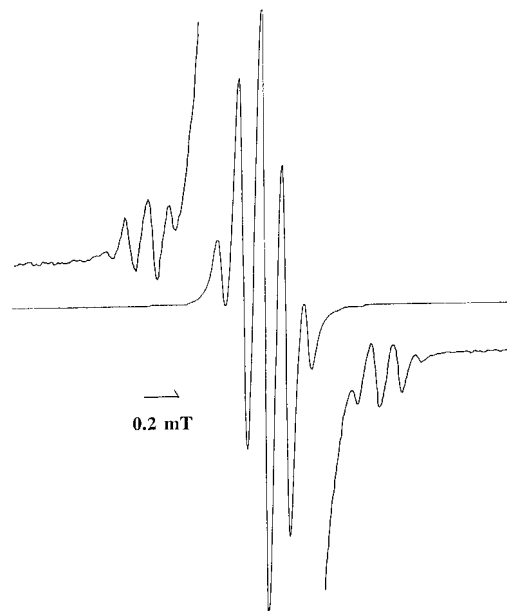


**Figure 3.** ESR spectrum of **1** oxidized by AgClO<sub>4</sub> in CH<sub>2</sub>Cl<sub>2</sub> at room temperature. On both sides the spectrum was amplified 50-fold, which is attributed to the <sup>33</sup>S hf structure

both TTS moieties, that is, a monocation radical state. However, it has been reported that iodine oxidation or charge-transfer complexation in our systems can proceed to the dicationic radical states and show a fine structure.<sup>9</sup> In our experiments, such spin–spin interaction is also envisaged, as discussed later.) In addition, the weak side lines support the present analysis. An isotropic hf interaction due to the sulfur atoms, <sup>33</sup>S ( $I = 3/2$ ), was observable as satellite lines in several TTF cation radicals, and in some cases the analyses were unambiguous and straightforward.<sup>10</sup> In the vinyl-bridged dications the main splitting and the <sup>33</sup>S satellite lines could be also observed, the spectral analysis giving a <sup>33</sup>S hfcc of 0.25 mT. The inner- and outermost components of the <sup>33</sup>S quartet splitting bear the same <sup>1</sup>H hf pattern as the central main one. It is emphasized that the <sup>33</sup>S hfcc value obtained is, again, almost half of the <sup>33</sup>S hfcc of TTF cation radical (0.427 mT).<sup>10</sup> This quantitative comparison of the <sup>33</sup>S satellite lines also assures the exchange interaction between the two TTFs.

The temperature dependences of the main splitting pattern are depicted in Fig. 4. The spectral intensity gradually decreases with decrease in temperature, implying a singlet ground state in this exchange coupled system. In the lower temperature region before solvent freezing, the spectrum seems to become changeable and evolve into a 1:3:3:1 pattern, which is typical of a non-interacting TTF cation radical.<sup>2,8</sup> This phenomenon is explained by assuming a hindered molecular configuration, especially in the two TTF groups in the solidified state, and thereby reduced spin–spin interaction. A non-interacting 1:3:3:1 pattern is evidenced by an almost

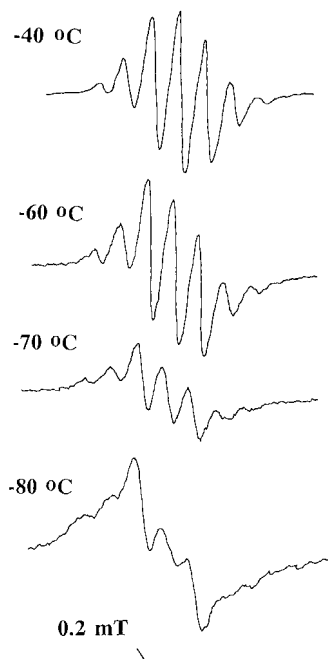


**Figure 4.** Temperature-dependent ESR spectra of **1**. Temperature is decreased from room temperature shown in Fig. 3

doubled hfcc compared with that of the seven-line pattern. The temperature variation, however, is reversible, so that higher temperature favors the two-TTF configuration in such a way as probably to result in exchange coupling between the two TTFs. This observation is compatible with the conclusion drawn for the carbonyl-bridged TTFs that the spin–spin coupling between the two unpaired electrons on each TTF group is strongly dependent on the medium (solvent or frozen solution), where the geometries are strikingly different.<sup>8</sup>

Further oxidation reaction from the doubly oxidized state gradually proceeds at room temperature in the  $\text{AgClO}_4\text{-CH}_2\text{Cl}_2$  system, as is indicated in Fig. 5. This does not necessarily substantiate further oxidation, that is, the third oxidation, but rather the time profile of the spectral change. This indicates the conformational change of the present radical species as is observed in the temperature variation. At any rate, the spectral change is interesting, in particular, for the  $^{33}\text{S}$  hf spectra. Figure 5(c) was taken 1 day after the reaction, which is a typical 1:3:3:1 pattern with a  $^1\text{H}$  hfcc of 0.12 mT, in which, correspondingly, a new  $^{33}\text{S}$  pattern with an hfcc of 0.5 mT also emerges. Both of the hfcc values in the final paramagnetic state are precisely doubled as compared with the initial seven-line state. Therefore, this pattern is the same as that of the non-interacting TTF species and similar to that of the TTF cation monoradical. In the intermediate time, the two species (seven- and four-line components) co-exist, as shown in Fig. 5(b). Although it is difficult to draw this conclusion quantitatively from the central main lines, the two types of  $^{33}\text{S}$  hf splitting

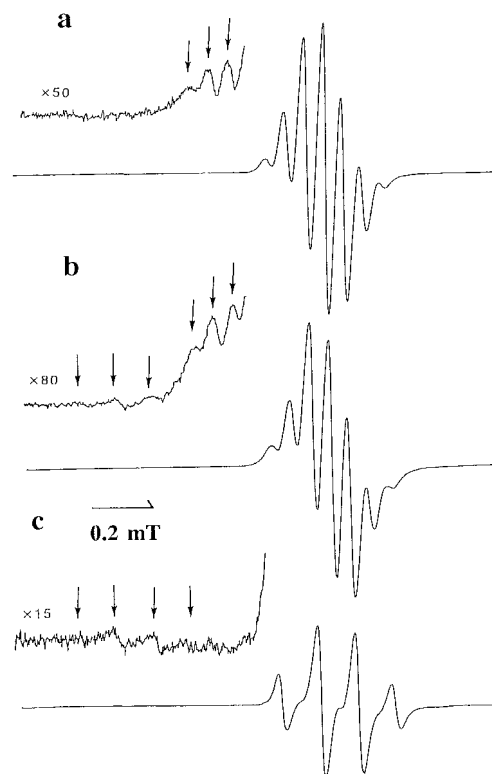


**Figure 5.** Time evolution of the cation radical species as revealed by ESR spectra. (a) Just after the reaction; (b) intermediate; (c) long-term oxidation reaction (more than 1 h) or a final yield product after leaving (a) overnight

separately appear and are assigned to interacting and non-interacting dication species, the spectral intensity being proportional to each radical state.

The temperature and time variations for **2** are almost the same as those for **1**. In the case of **3**, the spectrum obtained [Fig. 6(a)] was complicated because of the  $^1\text{H}$  hf splitting due to the methyl groups in the vinyl 2,2-positions. Utilizing the smallest splitting of 0.021 mT by the six methyl protons, we simulated the seven- and four-line structures. The results are a partially resolved broad absorption and a broad 1:3:3:1 pattern with unresolved splittings, respectively (Fig. 7). In the former simulation, the characteristic seven-line pattern disappears, leading to an inhomogeneously hf-broadened spectrum. Next, these fundamental absorptions were mixed in order to produce the observed pattern. The final satisfactory simulation was implemented using a mixing ratio of 10:3, as is shown in Fig. 6(b). A comparatively large amount of the mixing of the four-line structure in **3** implies an easier conformational change. The time profile of the spectra also indicates the dominant contribution of the four-line structure, on a much shorter time-scale than that for **1** or **2**.

Next we discuss triplet fine structures in the frozen solution at liquid-nitrogen temperature. Spin–spin interactions forming a triplet state generally give rise to fine structure splittings in rigid media, resulting in the

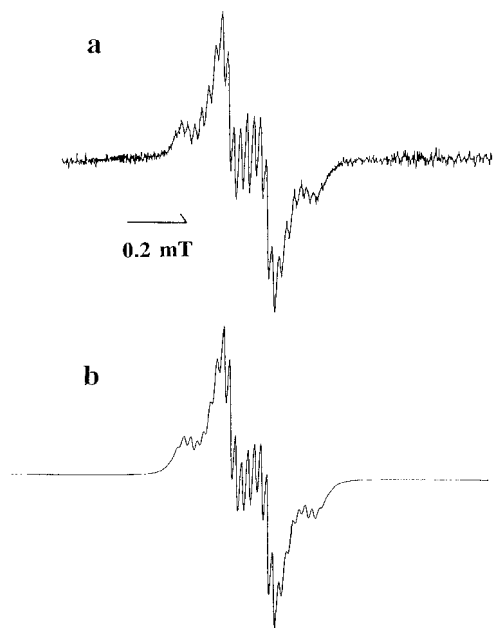


**Figure 6.** (a) ESR spectrum of **3** and (b) simulated spectrum (see text)

evaluation of zero-field splitting parameters,  $D$  and  $E$ .<sup>11</sup> This experiment provided uncontroversial evidence for the two-electron oxidation process and, therefore, the dicationic radical state. Actually, **2** and **3** displayed axial  $D$  and  $2D$  splittings, as is indicated by arrows in Fig. 8. The magnitude of the zero-field splitting parameter  $D$  was 2.8 mT, almost the same for **2** and **3**. The triplet spin state can also be ascertained by the observation of a double-quantum transition, which appears at half of the magnetic field center of the fine-structure absorption. This half-field resonance is usually forbidden, so that its absorption intensity is very weak. Through magnified amplitudes of the measurements, however, we could detect it for both **2** and **3**. Hence both the fine structure and the half-field resonance evidently support the triplet entity and spin-spin interaction in the doubly oxidized dimeric TTF in the frozen solution, causing the characteristic seven hf lines in solution.

However, it is noted that **1** did not manifest either such a fine structure or a half-field resonance under the same experimental conditions. In this case we cannot deny the

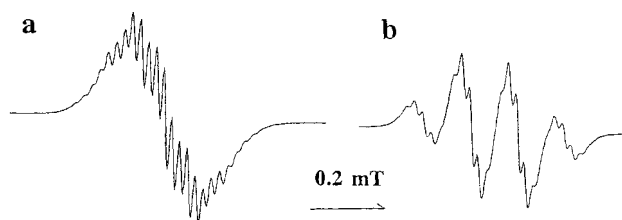


**Figure 7.** Simulated ESR spectra of **3** with (a) the seven-line and (b) the four-line hf-structure. Two methyl splittings are added (see text)

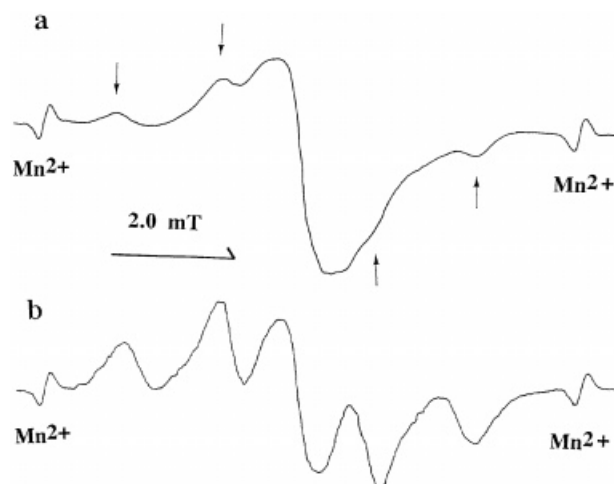
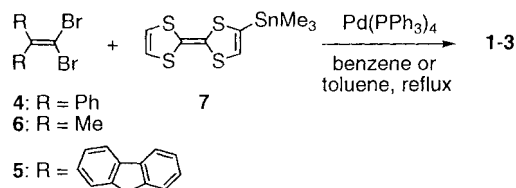


**Figure 8.** Fine-structure spectra of (a) **2** and (b) **3** quenched at 77 K immediately after the oxidation reaction at room temperature. The arrows in (a) indicate the  $2D$  and  $D$  separated components in the usual fine structure ( $D = 2.8$  mT). The sharp absorptions on both sides are due to  $\text{Mn}^{2+}$  standard

possibility of a one-electron oxidation reaction. However, in **2** and **3** the two-electron oxidation in the  $\text{AgClO}_4$  reaction was ascertained by the above-mentioned fine structure ( $S = 1$ ). Considering that the first redox potential (two-electron process) for **1** is lower than that for **2** and almost the same as that for **3**, the chemical reaction can proceed similarly to those for **2** and **3**, and therefore it is highly likely that the two-electron oxidized species will be obtained. In this respect, some comments are necessary. As shown in Fig. 4, lowering the temperature seems to cause a molecular configurational change which reduces the spin-spin interaction. Accordingly, one of the reasons is that the sterically hindered structure with less exchange interaction between the TTFs was quenched during the solidification of the solvent. This property might be relevant to the difference in the substituents at the 2,2-positions, namely two phenyls, planar fluorenyl and two small methyls. Compound **1** may be likely to reduce  $\pi$ -orbital interactions owing to the high flexibility of the molecular conformations as revealed by x-ray structure analysis (Fig. 1). The geometries of the TTF dimers are, in some details, discussed without considering the 2,2-substituents.<sup>6</sup>

The characteristic seven-line ESR patterns obtained for **1–3** in solution are essentially important as an implication of the spin-spin interaction between the two TTFs in our systems. Many conjugate compounds containing two or more TTF moieties have been prepared and the spin interactions have been examined. However, there are no examples, except for our cases, exhibiting evident hf structures of the interacting TTFs. The unpaired electron always resides on or is localized only on the TTF moiety, even in simply or directly coupled



Scheme 3

TTFs in which the interaction would be highly plausible. Regardless of the theoretical predictions for some TTF dimers,<sup>6</sup> the present study could not show the ground triplet state predicted for vinyl-bridged TTFs, but it demonstrated the typical hf pattern of the interacting TTFs and confirmed the possibility of the spin–spin interactions in the TTF oligomers.

## EXPERIMENTAL

**Materials.** The syntheses of **1–3** were carried out using the palladium-catalyzed cross-coupling reaction of 4-trimethylstannyl-TTF (**7**) with 2,2-disubstituted 1,1-dibromoethylenes (**4–6**) (Scheme 3).<sup>9,12,13</sup> As reported previously, the Stille reaction of **7** with **4–6** in refluxing benzene or toluene proceeded smoothly to produce the corresponding bis(tetrathiafulvalenyl)ethylenes **1–3** in moderate yields.

**X-ray structure analysis of 1.** Single crystals of **1** suitable for x-ray structure analysis were obtained by slow recrystallization; dark red prisms of crystal size  $0.20 \times 0.20 \times 0.60$  mm; intensity data were collected using a Rigaku 7R four-circle diffractometer with graphite-monochromated Mo K $\alpha$  radiation ( $I = 0.71069$ ; crystal system triclinic, space group *P1*; cell parameters:  $a = 10.171(1)$ ,  $b = 21.257(2)$ ,  $c = 6.3169(8)$ ,  $\alpha = 93.196(8)$ ,  $\beta = 100.66(1)$ ,  $\gamma = 102.074(8)$ ;  $V = 1306.2(3)$ ;  $Z = 2$ ;  $D_{\text{calcd}} = 1.487 \text{ g cm}^{-3}$ ;  $F_{000} = 600.00$ ;  $m(\text{MoK}\alpha) = 6.99 \text{ cm}^{-1}$ ; No. of unique reflections = 6040 ( $R_{\text{int}} = 0.014$ ); No. of reflections measured with  $I > 3.00\sigma(I) = 4392$ ;  $R = 0.038$ ,  $R_w = 0.027$ . Structural parameters of non-hydrogen atoms were refined anisotropically according to the full-matrix least-squares technique. Crystallographic data (excluding structure factors) for the structure **1** have been deposited with the Cambridge Crystallographic Data Centre as supplementary publication. Copies of the data can be obtained free of charge on application to The Director, CCDC, 12 Union Road, Cambridge CB2 1EZ, UK [Fax, +44 1223 336033; E-mail, deposit@chemchrys.cam.ac.uk].

**Cyclic voltammetry.** All electrochemical studies were performed using a BAS CV-27 voltammetric analyzer, which was equipped with a platinum electrode (1.6 or 3 mm diameter) as a working electrode, a standard Ag/Ag<sup>+</sup> reference electrode and a platinum wire counter electrode. The measurements were carried out on degassed anhydrous benzonitrile solution containing the sample (0.5–1 mM) and tetrabutylammonium perchlorate (0.1 M) as supporting electrolyte at 300 K. Cyclic voltammograms were scanned at a sweep rate of about  $100 \text{ mV s}^{-1}$ . Oxidation potentials are referred to ferrocene; Cp<sub>2</sub>Fe<sup>+0</sup> was set to 0.31 V.

**ESR measurements.** ESR measurements were carried out using a JEOL PX1050 or FE3X ESR spectrometer at the X-band with 100 kHz field modulation. Temperature was controlled by a JEOL DVT2 within an accuracy of 0.5 K. Magnetic field and hyperfine or fine splitting were calibrated by monitoring Mn<sup>2+</sup> signals in MgO. Cation radicals were obtained by electrochemical reactions and/or chemical oxidations (several oxidizing reagents were tried but we found AgClO<sub>4</sub> to be the most appropriate in CH<sub>2</sub>Cl<sub>2</sub> solutions).

## REFERENCES

- (a) Alivisatos AP, Barbara PE, Castleman AW, Chang J, Dixon DA, Klein ML, McLendon GL, Miller JS, Ratner MA, Rossky PJ, Stupp SI, Thompson ME. *Adv. Mater.* 1998; **10**: 1297; (b) Miller JS. *Adv. Mater.* 1998; **10**: 1553; (c) Ouahab L. *Chem. Mater.* 1997; **9**: 1909; (d) Enoki T, Yamaura J, Miyazaki A. *Bull. Chem. Soc. Jpn.* 1997; **70**: 2005; (e) Day P, Kurmoo M. *J. Mater. Chem.*, 1997; **7**: 1291.
- (a) Wudl F, Smith GM, Hufnagel EJ. *J. Chem. Soc., Chem. Commun.* 1970; 1453; (b) Ferraris J, Cowan DO, Walatka VV, Perlstein H. *J. Am. Chem. Soc.* 1973; **94**: 948.
- Yoshida Z, Sugimoto T. *Angew. Chem., Int. Ed. Engl.* 1988; **27**: 1573.
- Adam M, Mullen K. *Adv. Mater.* 1994; **6**: 439.
- Otsubo T, Aso Y, Takimiya K. *Adv. Mater.* 1996; **8**: 203.
- Mizoguchi H, Ikawa A, Fukutome H. *J. Am. Chem. Soc.* 1995; **117**: 3260.
- Lahti PM, Ichimura AS. *J. Org. Chem.* 1991; **56**: 3030.
- Sugimoto T, Yamaga S, Nakai M, Nakatsuji H, Yamauchi J, Fujita H, Fukutome H, Ikawa A, Mizoguchi H, Kai Y, Kanehisa N. *Adv. Mater.* 1993; **5**: 741.
- Iyoda M, Sasaki S, Miura M, Fukuda M, Yamauchi J. *Tetrahedron Lett.* 1999; **40**: 2807.
- Terahara A, Nishiguchi HO, Hirota N, Awaji H, Kawase T, Yoneda S, Sugimoto T, Yoshida Z. *Bull. Chem. Soc. Jpn.* 1984; **57**: 1760.
- Wertz JE, Bolton JR. *Electron Spin Resonance, Elementary Theory and Practical Applications*. Chapman and Hall: London, 1986.
- Iyoda M, Kuwatani Y, Ueno N, Oda M. *J. Chem. Soc., Chem. Commun.* 1992; 158.
- Iyoda M, Fukuda M, Yoshida M, Sasaki S. *Chem. Lett.* 1994; 2369.